

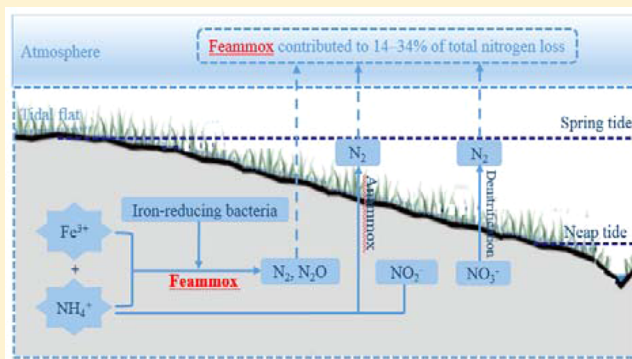
Evidence of Nitrogen Loss from Anaerobic Ammonium Oxidation Coupled with Ferric Iron Reduction in an Intertidal Wetland

Xiaofei Li,^{†,§} Lijun Hou,^{*,‡,§} Min Liu,^{*,†} Yanling Zheng,[‡] Guoyu Yin,[‡] Xianbiao Lin,[†] Lv Cheng,[†] Ye Li,[†] and Xiaoting Hu[†]

[†]College of Geographical Sciences, and [‡]State Key Laboratory of Estuarine and Coastal Research, East China Normal University, 3663 North Zhongshan Road, Shanghai 200062, China

S Supporting Information

ABSTRACT: Anaerobic ammonium oxidation coupled with nitrite reduction is an important microbial pathway of nitrogen removal in intertidal wetlands. However, little is known about the role of anaerobic ammonium oxidation coupled with ferric iron reduction (termed Feammox) in intertidal nitrogen cycling. In this study, sediment slurry incubation experiments were combined with an isotope-tracing technique to examine the dynamics of Feammox and its association with tidal fluctuations in the intertidal wetland of the Yangtze Estuary. Feammox was detected in the intertidal wetland sediments, with potential rates of 0.24–0.36 mg N kg⁻¹ d⁻¹. The Feammox rates in the sediments were generally higher during spring tides than during neap tides. The tidal fluctuations affected the growth of iron-reducing bacteria and reduction of ferric iron, which mediated Feammox activity and the associated nitrogen loss from intertidal wetlands to the atmosphere. An estimated loss of 11.5–18 t N km⁻² year⁻¹ was linked to Feammox, accounting for approximately 3.1–4.9% of the total external inorganic nitrogen transported into the Yangtze Estuary wetland each year. Overall, the co-occurrence of ferric iron reduction and ammonium oxidation suggests that Feammox can act as an ammonium removal mechanism in intertidal wetlands.



1. INTRODUCTION

Nitrogen (N) pollution in aquatic ecosystems has become a more significant environmental issue at regional and global scales,^{1–3} mainly due to the excessive use of N fertilizers in agricultural activities^{4,5} and to the release of N from fossil fuel combustion.^{2,4} Specifically, the substantial amount of N released into aquatic environments is considered an important driver of water pollution (e.g., coastal eutrophication, hypoxia, and harmful algal blooms).^{2,3,6–8} Shifts in microbial communities and diversity in response to N inputs⁹ also likely influence N transformations.¹⁰ Therefore, increasing concerns regarding the pathways of N cycling in aquatic environments have been raised for decades and can be used to help reveal N budgets in natural ecosystems and provide a thorough understanding of global N biogeochemistry.^{1,2} Of the N transformation processes, canonical denitrification, which is the heterotrophic reduction of nitrate to N₂, has traditionally been considered the only important mechanism of N loss from aquatic ecosystems.^{1,2,11} However, in recent years, anaerobic ammonium oxidation (anammox), which oxidizes ammonium into dinitrogen gas by reducing nitrite,^{12,13} has been found to contribute to the removal of N from freshwater, estuaries, and coastal marine environments.^{12–17} More recently, anaerobic ammonium oxidation coupled with Fe(III) reduction (termed Feammox), which can produce N₂,^{5,18} NO₃⁻,^{5,18} or

NO₂⁻,^{5,18–20} has been identified in many ecosystems including riparian sediments,^{19,20} tropical forest soils,¹⁸ and paddy soils.⁵ Because the production of N₂ by Feammox is more energetically favorable than the generation of NO₂⁻ or NO₃⁻,¹⁸ this process is considered a potentially significant contributor to N removal.^{5,18} However, no reports regarding the occurrence of Feammox or its contribution to total N losses are currently available for intertidal wetlands.

Intertidal wetlands are key transitional zones between land and marine ecosystems, play an important role in global biogeochemical cycles, and provide extensive ecosystem services.^{21–24} However, intertidal wetlands are usually subjected to periodic water inundation and atmospheric exposure due to tidal fluctuations.²⁷ In such environmental systems, sediments endure periodic desiccation, especially during neap tides, which can result in the oxidation of Fe(II) to Fe(III) and of ammonium to nitrite and nitrate. After desiccation, the rewetting of sediments during spring tides can contribute to Fe(III) reduction and to the generation of sedimentary ammonium through organic matter mineralization or ion

Received: July 14, 2015

Revised: September 2, 2015

Accepted: September 11, 2015

Published: September 11, 2015

exchange.^{25,26} In addition, changes between dry and wet processes can alter the sediment structure and sedimentary microenvironments.²⁷ Overall, alternant processes, such as the results of tidal fluctuations, can cause a series of interrelated biotic and abiotic changes that can affect biogeochemical reactions in intertidal wetlands.^{27,28} Considering the environmental characteristics of intertidal wetlands,^{8,27} we hypothesize that the periodic dry and wet processes induced by spring and neap tidal fluctuations can facilitate the microbial process of Feammox in these environments.

In this study, we provide geochemical evidence for Feammox in surface sediments from the intertidal wetland of the Yangtze Estuary. The main objective of this study is to examine the occurrence of Feammox and the associations of Feammox dynamics with sedimentary inorganic nitrogen changes and Fe redox reactions under tidal fluctuations. The abundance of iron-reducing bacteria (FeRB) which regulate Fe(III) reduction was measured. Furthermore, the contribution of Feammox to the total N loss from the intertidal wetland was identified. This work provides new insights regarding nitrogen biogeochemical cycles coupled with Fe redox reactions in intertidal wetlands.

2. MATERIALS AND METHODS

Site Description and Sediment Sampling. The Yangtze Estuary is located in the center of China's eastern coast. Extensive intertidal mudflats have developed along the Yangtze estuarine and coastal zone due to the deposition of substantial amounts of suspended sediment from the Yangtze River Basin.^{29,30} In this work, the research site (121°59'E, 31°30'N) was located in the Chongming Eastern Intertidal Wetland which is the largest and most extensively developed mudflat in the mouth of the Yangtze Estuary (Figure S1, [Supporting Information](#)). Because of semilunar tidal fluctuations, the inundation duration in this intertidal wetland can be maintained for approximately 3–5 d during spring tide. In contrast, this area is continuously exposed to air for approximately 10–12 d during intermediate and neap tides. Thus, these sediments in the intertidal wetland experience periodic dry and wet processes during semilunar tidal cycles, and this intertidal wetland was consequently selected as the case-study site. Fieldwork was conducted at the end of the spring and neap tides for two successive semilunar tidal cycles in August and December 2014, respectively. At each sampling, six replicates of sediment samples (0–5 cm depth) were collected from 3 m² of homogeneous intertidal mudflat using plexiglass corers. After collection, the sediment core samples were packed into cleaned polyethylene bags and sealed without air before transporting on ice to the laboratory within 2 h. After returning to the laboratory, each sediment core was immediately homogenized under helium and divided into three fractions. The first fraction was immediately incubated to determine the potential nitrogen transformation rates using isotope tracer incubations, the second fraction was stored at –80 °C for molecular analyses, and the third fraction was stored at 4 °C for sediment characteristics measurements, including the sediment water content, pH, redox potential, total organic carbon content, sedimentary inorganic nitrogen content, and reactive Fe concentrations.

Isotopic Tracer Incubations. Sediment slurry incubations combined with nitrogen isotope-tracing technique were conducted in an anaerobic glovebox to measure Feammox and Fe(III) reduction rates using the procedure from Ding et al.⁵ and Yang et al.¹⁸ with slight modifications. Briefly, slurries

were made by adding sterile anoxic artificial seawater (salinity: 10‰) to sediments at a ratio of 2:1 (v/w) and adequately homogenized using a magnetic stirrer before anaerobic preincubation in the dark at nearly in situ temperatures (30 °C for August and 10 °C for December) for approximately 12 h to eliminate background nitrite, nitrate, and oxygen. After preincubation, 12 g of the homogenized slurries were transferred into 100 mL serum vials under helium before immediately sealing the vials with butyl rubber septa and crimp-capping with aluminum caps. These vials were divided into the three following treatments: (1) sterile anoxic artificial seawater instead of ¹⁵NH₄Cl (control); (2) ¹⁵NH₄Cl addition (¹⁵N at 99.0%, Cambridge Isotope Laboratories, Inc., Tewksbury, MA, ¹⁵NH₄⁺); and (3) ¹⁵NH₄Cl and C₂H₂ addition (¹⁵NH₄⁺ + C₂H₂). The vials for both ¹⁵NH₄⁺ and ¹⁵NH₄⁺ + C₂H₂ treatments were spiked with 1.0 mL of ultrahigh purity He-purged stock solutions of ¹⁵NH₄Cl through the septa to achieve a dry weight of 45 mg N kg⁻¹, which was based on the annual inorganic N (IN) load into the Yangtze Estuary wetlands.²¹ For the ¹⁵NH₄⁺ + C₂H₂ treatments, 30 mL of headspace gas in each vial was replaced with C₂H₂. All vials were vigorously shaken to homogenize the treatment solutions before incubation. After 24 h of incubation, 12 mL of gas samples were collected immediately using gastight syringes and then injected into 12 mL pre-evacuated Labco Exetainer vials sealed with butyl-rubber septa (Labco Limited, High Wycombe, Buckinghamshire, U.K.). The ¹⁵N enrichment of N₂ in the gas samples was determined using an isotope ratio mass spectrometry (IRMS, Thermo Finnigan Delta V Advantage, Bremen, Germany), and a more detailed description is provided in the [Supporting Information](#). The potential Feammox rates were conservatively quantified using the difference in ³⁰N₂ production with and without ¹⁵NH₄⁺ addition.⁵ Furthermore, after the gas samples were collected to determinate the Feammox rates, the incubated slurries were also immediately subsampled to quantify the Fe(III) reduction rates based on changes in the Fe(II) concentration during the incubations.⁵

Analysis of Sediment Characteristics. The sediment water content was determined from the amount of weight lost from a known amount of wet sediment that had been dried at 60 °C to a constant value. The redox potential (Eh) of the sediment was measured using a combined Ag/AgCl and Pt (s) electrode connected to a potentiometer, and Zobell solution was used for calibration.²⁷ The sediment pH was measured using a Mettler-Toledo pH meter after mixing the sediment with deionized water free of CO₂ at a ratio (w/v) of 1:2.5.²¹ The total organic carbon (TOC) in sediments was determined using a thermal combustion furnace analyzer (Elementar vario MaxCNOHS analyzer, Germany) after leaching with 1 M HCl to remove carbonate.²¹ The exchangeable NH₄⁺, NO₃⁻, and NO₂⁻ in the sediments were extracted using a 2 M KCl solution and determined via a continuous-flow nutrient autoanalyzer (SAN plus, Skalar Analytical B.V., Breda, The Netherlands) with detection limits of 0.5 μM for NH₄⁺ and 0.1 μM for NO₃⁻ and NO₂⁻.²¹ The total extractable Fe and Fe(II) in the sediments were determined using the procedure described by Lovley et al.³¹ with slight modifications. Briefly, 1.0 g samples were extracted in 10 mL mixtures of 0.5 M HCl and 0.25 M hydroxylamine hydrochloride for 2 h to determine the total extractable Fe and Fe(II), respectively, using the ferrozine method.³¹ The amount of microbially reducible Fe(III) (considered as hydroxylamine-reducible Fe(III)) was

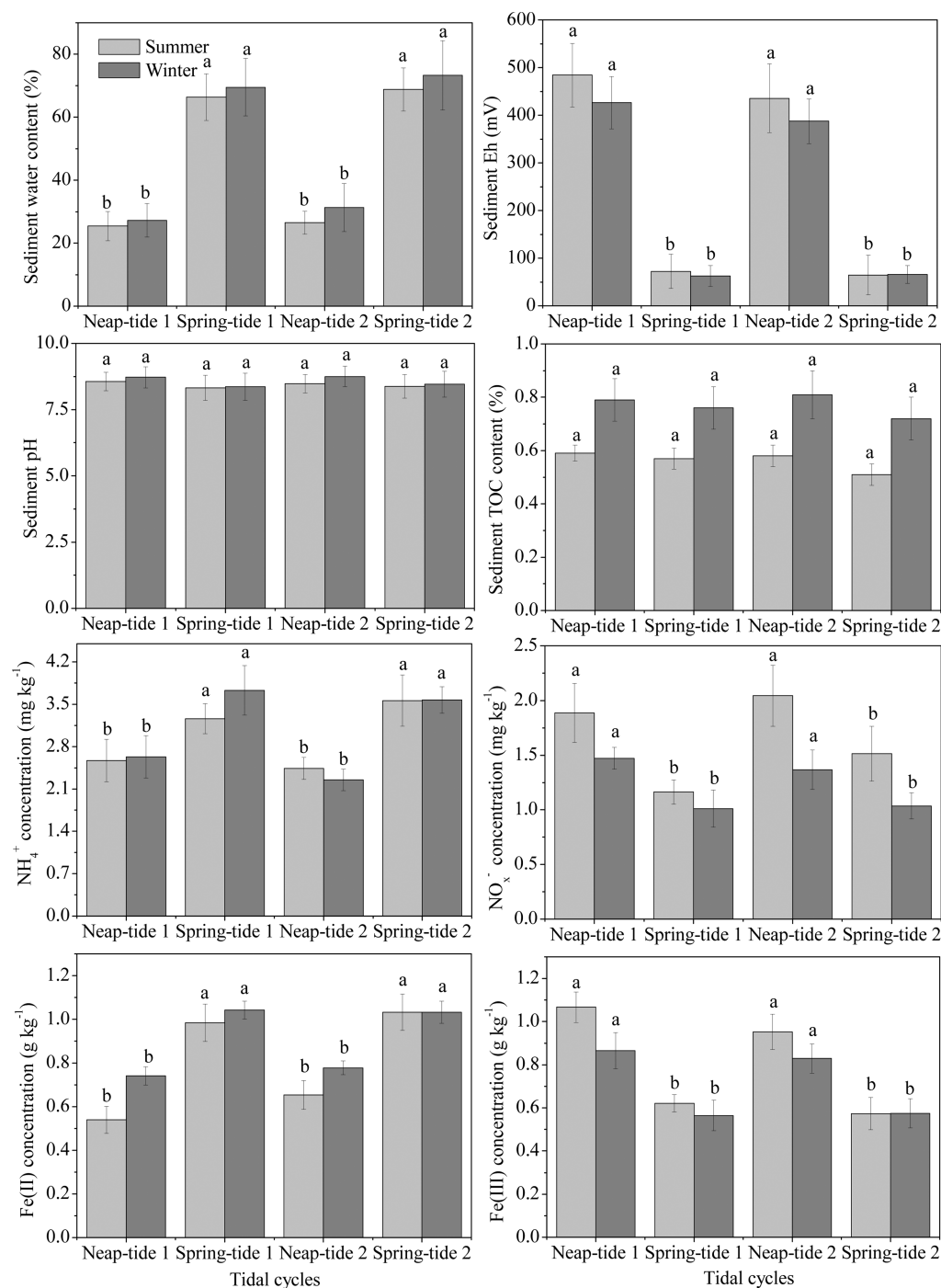


Figure 1. Dynamics of water content, Eh, pH, TOC, exchanged inorganic nitrogen, Fe(II), and Fe(III) in sediments collected at the two successive spring and neap tides in summer and winter, respectively. $\text{NO}_x^- = \text{NO}_3^- + \text{NO}_2^-$. The different small letters above the column denote statistically significant ($P < 0.05$) differences between the spring and neap tides in summer and winter. Error bars represent standard errors ($n = 6$).

calculated as the difference between the total extractable Fe and Fe(II).^{5,31}

DNA Extraction and PCR Amplification. The total genomic DNA of the sediment was extracted from 0.25 g of sediment and sampled using Power Soil DNA Isolation kits (MoBio, U.S.A.) according to the manufacturer's directions.^{7,21} The purities and concentrations of DNA were measured on a Nanodrop-2000 Spectrophotometer (Thermo, U.S.A.). Quantitative PCR (qPCR) of the iron-reducing bacteria (FeRB) was performed using the specific primer sets and qPCR conditions reported by Somenahally et al.³² FeRB was determined by

targeting *Geobacteraceae* spp. and *Shewanella* spp., which are important microbial communities involved in iron reduction under anaerobic conditions.³² The *Geobacteraceae* fragments in the extracted DNA were amplified using the Geo564F (5'-AAG CGT TGT TCG GAW TTA T-3') and Geo840R (5'-GGC ACT GCA GG GGT CAA T A-3') primers. The *Shewanella* fragments were amplified using the She 120F (5'-GCC TAG GGA TCT GCC CAG TCG-3') and She 220R (5'-CTA GGT TCA TCC AAT CGC G -3') primers. In addition, qPCR was conducted using an ABI 7500 Sequence Detection System (Applied Biosystems, Canada) and the SYBR green qPCR

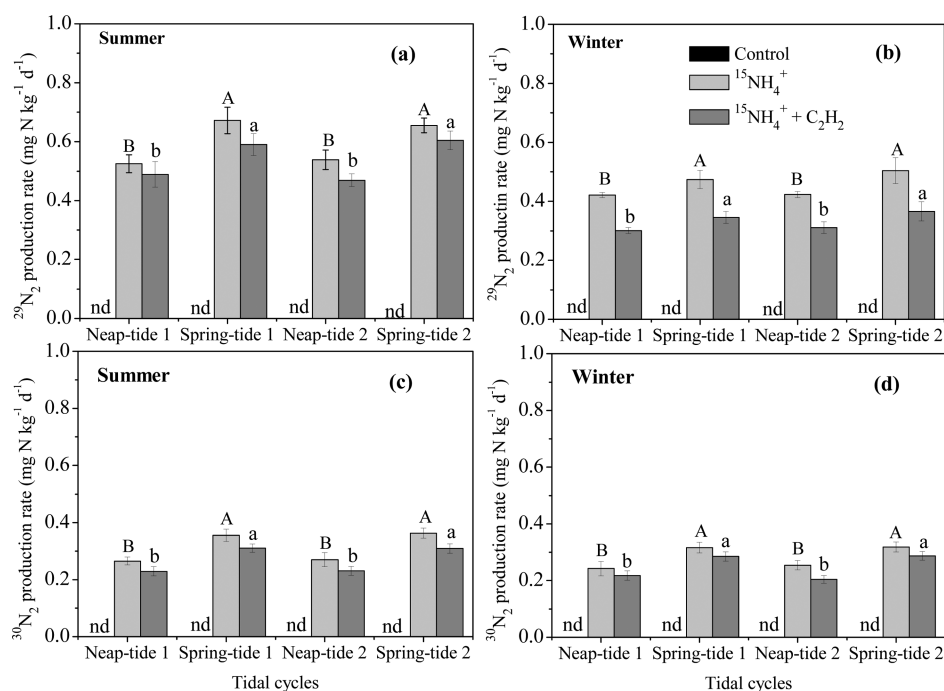


Figure 2. Mean $^{30}\text{N}_2$ and $^{29}\text{N}_2$ production rates in the control, $^{15}\text{NH}_4^+$ and $^{15}\text{NH}_4^+ + \text{C}_2\text{H}_2$ treatments for the sediments influenced by tidal fluctuations. The different capital and small letters above the column denote statistically significant ($P < 0.05$) differences between the spring and neap tides in the $^{15}\text{NH}_4^+$ and $^{15}\text{NH}_4^+ + \text{C}_2\text{H}_2$ treatments, respectively. Error bars represent standard errors ($n = 6$). nd = not detectable within a detection limit of $0.006 \text{ mg } ^{15}\text{N kg}^{-1} \text{ d}^{-1}$.

method.⁷ Additional detailed descriptions of the qPCR amplification for FeRB are provided in the [Supporting Information](#).

Statistical Analyses. All statistical analyses were performed using SPSS version 17.0 for Windows (SPSS Inc., Chicago, IL). Statistical analyses for comparing the obtained data during spring and neap tides were conducted using a one-way analysis of variance (ANOVA) followed by a LSD test. Pearson's correlation analysis was performed to reveal the relationships among the environmental factors, Fe(III) reduction rates, FeRB abundance, and nitrogen transformation rates.

3. RESULTS

Dynamics of the Sediment Characteristics. Changes in the sediment characteristics during the neap and spring tidal fluctuations are shown in [Figure 1](#). The sediment water contents were significantly higher during spring tides (66.4–73.3%) than during neap tides (25.4–31.3%) ($P < 0.01$). In contrast, the sediment Eh was significantly lower during spring tides (62.7–72.4 mV) than during neap tides (387.6–484.3 mV) ($P < 0.01$); the sediment pH was slightly lower during spring tides (8.32–8.46) than during neap tides (8.48–8.75), but no significant seasonal difference was observed ($P > 0.05$). The sediment TOC contents during the spring tides (0.51–0.76%) were comparable to those during the neap tides (0.58–0.81%) and were significantly lower (0.51–0.59%) during the summer than during the winter (0.72–0.81%) ($P < 0.05$). The sediment NH_4^+ concentrations generally increased during the spring tides (3.26–3.73 mg N kg^{-1}) and significantly decreased during the neap tides (2.25–2.63 mg N kg^{-1}) ($P < 0.01$). Compared with NH_4^+ , opposite changes in the sediment NO_x^- concentrations were observed during the periodic tidal fluctuations. The Fe(II) contents in the sediments varied from 0.54 to 1.03 g Fe kg^{-1} during the summer and from 0.74

to 1.04 g Fe kg^{-1} during the winter, and the Fe(III) contents varied from 0.57 to 1.07 g Fe kg^{-1} during the summer and from 0.57 to 0.87 g Fe kg^{-1} during the winter. Specifically, the Fe(II) contents increased significantly during the spring tides as the Fe(III) contents significantly decreased relative to the neap tides ($P < 0.01$).

$^{15}\text{N}_2$ Production Measured through Isotopic Tracer Incubations. The potential $^{30}\text{N}_2$ and $^{29}\text{N}_2$ production rates in intertidal sediments influenced by the spring and neap tides were determined using ^{15}N -labeled ammonium-based isotope tracing and acetylene inhibition techniques ([Figure 2](#)). Significant $^{30}\text{N}_2$ contents were detected in the treatments with both $^{15}\text{NH}_4^+$ and $^{15}\text{NH}_4^+ + \text{C}_2\text{H}_2$, but no $^{30}\text{N}_2$ was detected in the control treatments (without $^{15}\text{NH}_4^+$ addition). This result demonstrates the occurrence of Feammox in the intertidal sediments because the N_2 resulting directly from Feammox and/or Feammox-produced NO_3^- or NO_2^- , which resulted from denitrification or anammox after Feammox, are the only potential sources of $^{30}\text{N}_2$ under anoxic conditions.^{5,18} The mean $^{30}\text{N}_2$ production rates in the $^{15}\text{NH}_4^+$ treatments were significantly greater than those in the $^{15}\text{NH}_4^+ + \text{C}_2\text{H}_2$ treatments, regardless of seasonal changes or tidal fluctuations ($P < 0.05$; [Figure 2c, d](#)). In the $^{15}\text{NH}_4^+$ treatments, the mean $^{30}\text{N}_2$ production rates during the spring tides ranged from 0.35 to 0.36 $\text{mg N kg}^{-1} \text{ d}^{-1}$ in the summer and from 0.32 to 0.33 $\text{mg N kg}^{-1} \text{ d}^{-1}$ in the winter, which were significantly higher ($P < 0.05$) than the rates observed during the neap tides (0.26–0.27 $\text{mg N kg}^{-1} \text{ d}^{-1}$ in summer and 0.24–0.25 $\text{mg N kg}^{-1} \text{ d}^{-1}$ in winter). In contrast, the presence of C_2H_2 resulted in a decrease of 0.02–0.06 $\text{mg N kg}^{-1} \text{ d}^{-1}$ in the $^{30}\text{N}_2$ production rates. The $^{30}\text{N}_2$ production rates in the $^{15}\text{NH}_4^+ + \text{C}_2\text{H}_2$ treatments showed similar seasonal changes to those observed in the $^{15}\text{NH}_4^+$ treatments. The formation of $^{29}\text{N}_2$ in the sediments under the tidal fluctuations was approximately twofold greater than

that of $^{30}\text{N}_2$ (Figure 2a, b). During the isotope-tracing incubations treated with both $^{15}\text{NH}_4^+$ and $^{15}\text{NH}_4^+ + \text{C}_2\text{H}_2$, the $^{29}\text{N}_2$ production rates showed similar variations as the $^{30}\text{N}_2$ production rates.

Fe(III) Reduction Rates in Isotopic Tracer Incubations.

In this study, the Fe(III) reduction rates were significantly enhanced in the $^{15}\text{NH}_4^+$ and $^{15}\text{NH}_4^+ + \text{C}_2\text{H}_2$ treatments, compared with the rates observed in the control treatments ($P < 0.05$; Figure 3). Additionally, the increase in Fe(III)

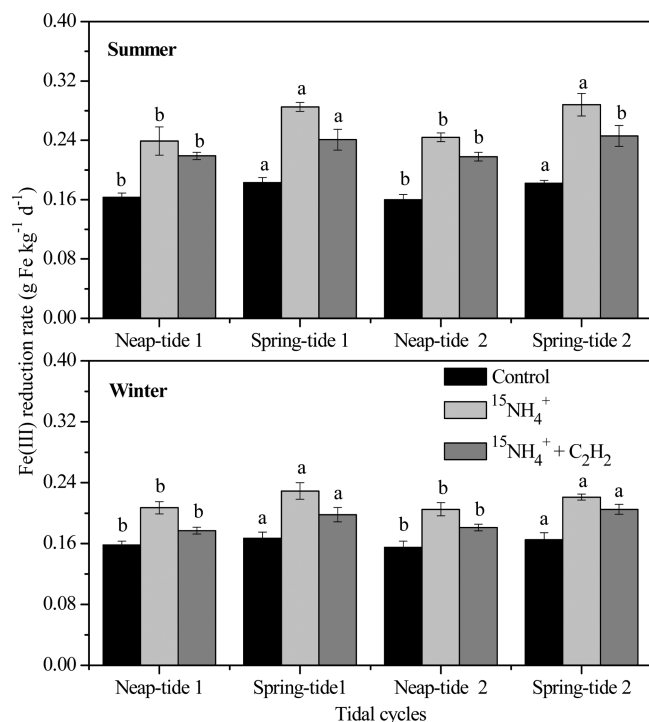


Figure 3. Fe(III) reduction rates measured through isotope tracer incubations. The different small letters above the column denote statistically significant ($P < 0.05$) differences between the spring and neap tides. Error bars represent standard errors ($n = 6$).

reduction rates was greater in the $^{15}\text{NH}_4^+$ treatments than in the $^{15}\text{NH}_4^+ + \text{C}_2\text{H}_2$ treatments ($P < 0.05$). These results indicate that a portion of the sedimentary indigenous Fe(III) was reduced to Fe(II) and that the addition of $^{15}\text{NH}_4^+$ facilitated Fe(III) reduction. The Fe(III) reduction rates were generally higher during the summer than during the winter ($P < 0.05$), likely because of the seasonal differences in temperature, sediment microbial communities, and/or sediment compositions. Moreover, in the $^{15}\text{NH}_4^+$ and $^{15}\text{NH}_4^+ + \text{C}_2\text{H}_2$ treatments, the Fe(III) reduction rates in the neap tidal sediments were greater during the summer ($0.21\text{--}0.24 \text{ g Fe kg}^{-1} \text{ d}^{-1}$) than during the winter ($0.19\text{--}0.21 \text{ g Fe kg}^{-1} \text{ d}^{-1}$) and increased by 31.0–52.5% and 18.4–36.3%, respectively, compared with the control treatments ($P < 0.05$). In the spring tidal sediments, the Fe(III) reduction rates during the summer ($0.23\text{--}0.29 \text{ g Fe kg}^{-1} \text{ d}^{-1}$) were significantly higher than those during the winter ($0.20\text{--}0.23 \text{ g Fe kg}^{-1} \text{ d}^{-1}$).

Abundance of Iron-Reducing Bacteria in Intertidal Sediments. The gene copy numbers of iron-reducing bacteria in the sediments under the tidal fluctuations were measured to demonstrate their activity, which may regulate Feammox (Figure 4). The abundance of *Geobacteraceae* spp. serves a significant role in iron reduction, varying from 1.0×10^8 to 1.4

$\times 10^8$ copies g^{-1} during neap tides and increasing significantly from 1.9×10^8 to 2.3×10^8 copies g^{-1} during spring tides ($P < 0.05$). Significant seasonal variations in the abundance of *Geobacteraceae* spp. occurred during the neap tides ($P < 0.05$), and no significant seasonal difference in *Geobacteraceae* spp. abundance was observed during the spring tides. The *Shewanella* spp. abundances during neap tides ranged from 1.5×10^7 to 1.9×10^7 copies g^{-1} and were lower than the abundances ($2.2 \times 10^7\text{--}3.7 \times 10^7$ copies g^{-1}) observed during spring tides (Figure 4). Furthermore, significant seasonal differences in the abundances of both *Geobacteraceae* spp. and *Shewanella* spp. were observed during spring tides ($P < 0.05$), while no seasonal differences were detected during neap tides ($P > 0.05$).

4. DISCUSSION

Occurrence of Feammox in Intertidal Wetlands. Tidal fluctuations can result in periodic changes in sediment characteristics, which can alter the microbial nitrogen transformation processes in the intertidal wetlands.³³ Nitrification, the sequential oxidation of NH_4^+ to NO_2^- and then to NO_3^- , is a dominant microbial process in aerobic environments.³⁵ However, under anaerobic conditions, the accumulation of NH_4^+ derived from organic nitrogen mineralization increases,³³ and NO_x^- is reduced by anammox and denitrification.⁵ In this study, significant differences in the sedimentary NO_x^- and NH_4^+ concentrations were detected between the spring and neap tidal sediments ($P < 0.05$) (Figure 1), which indicates the likely occurrence of tide-mediated microbial nitrogen transformations. In addition, Fe oxidation/reduction reactions can occur with tidal fluctuations, resulting in changes in the Fe(III) and/or Fe(II) concentrations in intertidal wetlands.³⁶ Fe(III), which serves as an electron acceptor, is widely available in intertidal wetlands and plays an important role in anaerobic organic matter oxidation³⁷ and microbial nitrogen cycling.¹⁹ In this study, the Fe(II) concentrations were significantly higher during the spring tides than during the neap tides. In contrast, Fe(III) concentrations were higher during the neap tides than during the spring tides. The changes in reactive Fe concentrations under these tidal fluctuations indicate that tidal action is an important factor regulating the Fe redox reactions in intertidal wetlands. Overall, these concurrent changes in sedimentary IN and reactive Fe concentrations induced by tidal fluctuations may be important for Feammox in intertidal wetlands.

Our isotopic experiments further demonstrated that Feammox occurred in the intertidal sediments, because significant $^{30}\text{N}_2$ production (Figure 2c, d) and high Fe(III) reduction (Figure 3) occurred following the addition of $^{15}\text{NH}_4^+$ in the treatments with $^{15}\text{NH}_4^+$ and $^{15}\text{NH}_4^+ + \text{C}_2\text{H}_2$. Furthermore, a significant and positive correlation was observed between the Fe(III) reduction and $^{30}\text{N}_2$ production rates ($P < 0.01$) (Figure 5), which supports the occurrence of Feammox in the intertidal sediments. Before the isotopic tracer incubations, the sediment slurries were anoxically incubated to eliminate initial NO_x^- and O_2 (Figure S2, Supporting Information). In addition, experimental procedures were conducted in an anaerobic glovebox filled with high-purity helium. Therefore, N_2 directly from Feammox and/or Feammox-produced NO_3^- or NO_2^- , which are produced by denitrification or anammox following Feammox, are the only potential pathways for $^{30}\text{N}_2$ generation.^{5,18}

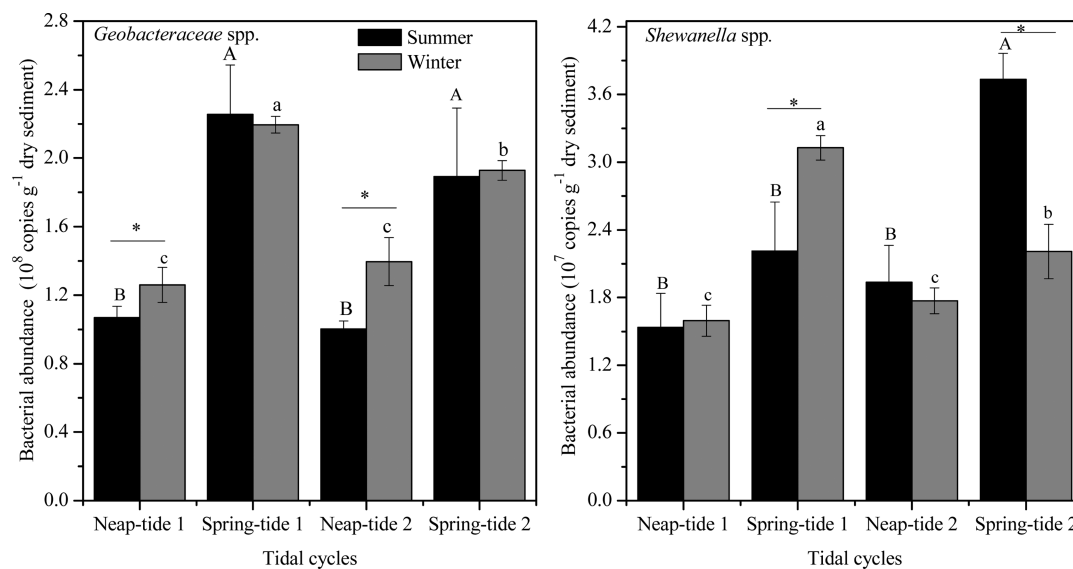


Figure 4. Gene copy numbers of *Geobacteraceae* spp. and *Shewanella* spp. bacteria in the sediments influenced by tidal fluctuations. The different capital and small letters above the column denote statistically significant ($P < 0.05$) differences between the spring and neap tides in summer and winter, respectively. The asterisks above the horizontal line denote statistically significant ($P < 0.05$) differences in seasonal variations. Error bars represent standard errors ($n = 6$).

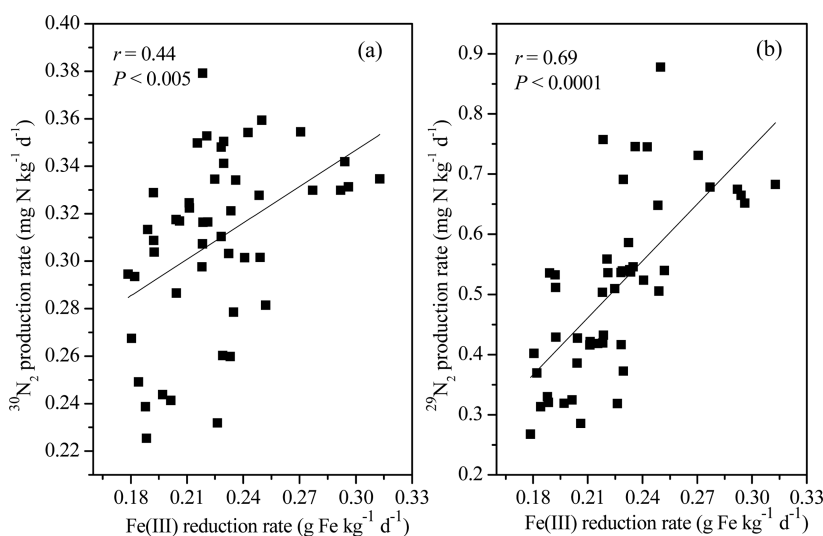


Figure 5. Pearson's correlations of iron reduction rates with both $^{30}\text{N}_2$ (a) and $^{29}\text{N}_2$ (b) production rates in the $^{15}\text{NH}_4^+$ treatment.

In this study, the potential Feammox rates estimated from $^{30}\text{N}_2$ production in the $^{15}\text{NH}_4^+$ treatments^{5,18} ranged from 0.24 to 0.36 mg N kg⁻¹ d⁻¹ (Figure 2c, d), which are comparable to the Feammox rates observed in tropical forest soils (approximately 0.32 mg N kg⁻¹ d⁻¹) by Yang et al.¹⁸ and in paddy soils (0.17–0.59 mg N kg⁻¹ d⁻¹) by Ding et al.⁵ Additionally, the estimated Feammox rates were significantly higher during the spring tides (0.32–0.36 mg N kg⁻¹ d⁻¹) than during the neap tides (0.24–0.27 mg N kg⁻¹ d⁻¹), which implies that tidal actions favor the occurrence of Feammox. Previous studies have revealed that Feammox reactions strongly depend on microbially reducible Fe(III) levels in soils.^{5,18–20} Likewise, a significant correlation was observed between the Feammox rates and Fe(III) concentrations in the present study ($r = 0.81$, $P < 0.01$), which indicates that the Feammox dynamics (Figure 2c, d) are likely attributable to the accumulation and/or reduction of Fe-oxides induced by tidal fluctuations. The Feammox process could also be affected by

pH and Eh^{5,18,19} because pH and Eh are important factors regulating the reactivity of Fe oxide minerals and Fe redox reactions.^{32,36,39} However, no significant relationship was observed between sediment pH and Feammox rates in this study ($r = -0.29$, $P > 0.05$), indicating that sediment pH may have a slight influence on Feammox reactions in intertidal wetlands. In contrast, the sediment Eh was significantly correlated with the Feammox rates ($r = -0.87$, $P < 0.01$). This relationship indicates that changes in sediment Eh may effectively control the conversion of Fe, which would drive the occurrence of Feammox. In addition, high concentrations of organic matter have been reported to increase the release of structural Fe from clay minerals and result in the formation of Fe(III) oxides, which would promote the Feammox reactions.⁵ Nevertheless, in this study, no significant relationship was observed between Feammox and TOC ($r = 0.34$, $P > 0.05$), which suggests that the availability of organic matter is not an important factor responsible for Feammox in intertidal

wetlands. Therefore, these results suggest that environments with high Fe(III)-oxide availability and low or fluctuating redox conditions are favorable for the occurrence of the microbial Feammox process.^{5,18–20}

Links among Fe(III) Reduction Rates, $^{15}\text{N}_2$ Production Rates, and Iron-Reducing Bacterial Abundance. Fe(III) reduction rates were significantly enhanced in the $^{15}\text{NH}_4^+$ and $^{15}\text{NH}_4^+ + \text{C}_2\text{H}_2$ treatments ($0.19\text{--}0.29 \text{ g Fe kg}^{-1} \text{ d}^{-1}$) relative to the control treatments ($0.16\text{--}0.18 \text{ g Fe kg}^{-1} \text{ d}^{-1}$) ($P < 0.05$; Figure 3), which indicates that the addition of NH_4^+ can facilitate Fe(III) reduction.⁵ Furthermore, the Fe(III) reduction rates varied significantly between the neap and spring tides, providing further evidence for the importance of tidal fluctuations in regulating the Fe redox reaction in intertidal sediments.^{34,35} Fe(III) availability and reduction rates can control the microbial Feammox process,^{5,18} mainly because Fe(III) can serve as an electron acceptor for organic matter degradation and ammonium oxidation under anaerobic conditions^{19,38} and stimulate the growth of iron-reducing bacteria.³⁹ Therefore, Fe(III) reduction could be associated with $^{30}\text{N}_2$ and $^{29}\text{N}_2$ production in the presence of $^{15}\text{NH}_4^+$. In this study, the Fe(III) reduction rates within the $^{15}\text{NH}_4^+$ -amended incubations were significantly correlated with both $^{30}\text{N}_2$ ($r = 0.44$, $P < 0.01$) and $^{29}\text{N}_2$ ($r = 0.69$, $P < 0.01$) production rates (Figure 5), further indicating that Feammox plays a significant role in anaerobic ammonium oxidation in intertidal wetlands. Considering the production of $^{29}\text{N}_2$ and $^{30}\text{N}_2$, anaerobic ammonium oxidation consumed 1.21–2.26% and 1.25–2.75% of the $^{15}\text{NH}_4^+$ added to the neap and spring tidal sediments, respectively.

Iron-reducing bacteria (FeRB) can affect Feammox by controlling Fe(III) reduction in anaerobic environments.^{32,39} The FeRB targeting *Geobacteraceae* spp. and *Shewanella* spp. that serve as Fe(III) reducers^{40,41} may be directly involved in ammonium oxidation.^{19,20} In this study, the abundances of *Geobacteraceae* spp. and *Shewanella* spp. were quantified to reveal the microbially physiological mechanisms underlying the interactions between Fe(III) reduction and Feammox. The Fe(III) reduction rates within the $^{15}\text{NH}_4^+$ -amended incubations were significantly related to the bacterial abundances of *Geobacteraceae* ($r = 0.52$, $P < 0.01$) and *Shewanella* ($r = 0.46$, $P < 0.01$) (Table S1, Supporting Information), as observed for the production of $^{30}\text{N}_2$ and $^{29}\text{N}_2$ vs reduction of Fe(III) (Figure 5). In addition, the $^{30}\text{N}_2$ production rates were significantly correlated with the bacterial abundances of *Geobacteraceae* ($r = 0.59$, $P < 0.01$) and *Shewanella* ($r = 0.57$, $P < 0.01$) (Table S1, Supporting Information). These relationships likely provide genetic evidence of the importance of microbially reducible Fe(III) in the occurrence of Feammox. The $^{30}\text{N}_2$ production rates were positively correlated with the $^{29}\text{N}_2$ production rates ($r = 0.66$, $P < 0.01$, Table S1, Supporting Information). This correlation likely indicates the concurrence of many microbial processes, including the use of indigenous $^{14}\text{NH}_4^+$ with added $^{15}\text{NH}_4^+$ by Feammox to form N_2 , Feammox to NO_3^- and/or NO_2^- followed by denitrification to N_2 , and Feammox to NO_2^- followed by anammox.^{5,18} This conclusion may also be supported by the weak correlations that were observed between the $^{29}\text{N}_2$ and $^{30}\text{N}_2$ production rates and denitrification and anammox bacterial abundances in this study (Figure S3, Supporting Information).

Compared with the neap tides, the high abundances of *Geobacteraceae* and *Shewanella* bacteria during the spring tides

indicate that the tidal fluctuations significantly influenced the growth of iron-reducing bacteria and impacted Feammox. The abundance of *Geobacteraceae* bacteria during the neap tides was higher during the summer than during the winter ($P < 0.01$), with no seasonal differences during the spring tides ($P > 0.05$). However, the abundance of *Shewanella* bacteria was higher during the spring tides than during the neap tides, and significant seasonal changes were observed during the spring tides ($P < 0.05$; Figure 4). These results indicate that FeRB had various physiological characteristics in response to the tidal fluctuations, which further affected the Feammox activity.^{32,39} However, some other microbial processes, such as anaerobic organic matter and methane oxidation,^{42,43} are also potential contributors to Fe(III) reduction,^{5,37,42} which may promote FeRB growth and metabolic activity.

Contribution of Feammox to Nitrogen Loss. To obtain the N_2 produced directly from Feammox, acetylene was added in the isotopic tracer incubations to directly separate the generation of N_2 via Feammox and/or denitrification of NO_3^- and NO_2^- produced from Feammox.^{5,18,44} Previous studies have indicated that acetylene not only restrains the reduction of N_2O produced from denitrification to N_2 ⁴⁵ but also inhibits anammox.^{5,44} In this study, the concentration of acetylene in the headspace of the serum vials reached up to 30% (v/v, about 12.78 mM), which could completely suppress N_2O reduction⁴⁵ and anammox.⁴⁴ Therefore, the N_2 produced directly from Feammox was considered the only microbial pathway of $^{30}\text{N}_2$ generation in the treatments of $^{15}\text{NH}_4^+ + \text{C}_2\text{H}_2$.^{5,18} Compared to the incubations treated only with $^{15}\text{NH}_4^+$, the decrease in $^{30}\text{N}_2$ production due to acetylene addition indicates that approximately 6.8–21.5% of the $^{30}\text{N}_2$ produced during the incubations was attributed to anammox and/or denitrification of Feammox-produced NO_2^- and NO_3^- .⁵ Therefore, the N_2 directly resulting from Feammox was estimated to account for 78.5 to 93.2% of the total $^{30}\text{N}_2$ production during the incubations in which only $^{15}\text{NH}_4^+$ was added. Based on the potential N_2O production rates in the presence of acetylene (Figure S4, Supporting Information), approximately $0.02\text{--}0.08 \text{ mg N kg}^{-1} \text{ d}^{-1}$ was oxidized by Fe(III) to NO_3^- and/or NO_2^- and then reduced to N_2O through denitrification,^{5,18} which accounted for 8.3–21.4% of the $^{30}\text{N}_2$ produced within the incubations. This proportion could also support the differences in $^{30}\text{N}_2$ generation with and without acetylene addition.

To identify the relative contributions of Feammox to nitrogen loss, the potential anammox and denitrification rates under the spring and neap tidal fluctuations were determined in the present study (Supplementary Methods, Supporting Information). The measured anammox and denitrification rates in the intertidal sediments ranged from 0.12 to 0.22 $\text{mg N kg}^{-1} \text{ d}^{-1}$ and from 0.41 to 1.68 $\text{mg N kg}^{-1} \text{ d}^{-1}$, respectively (Figure S5, Supporting Information). Based on the anammox and denitrification rates, Feammox accounted for 14–34% of the total nitrogen loss (sum of denitrification, anammox, and Feammox) through NH_4^+ oxidation coupled with Fe(III) reduction (Figure S6, Supporting Information).^{5,18} The remainder of the nitrogen loss was attributed to both denitrification and anammox. Additionally, Feammox resulted in slightly greater contributions to nitrogen loss during spring tides (16–34%) than during neap tides (14–30%), likely because relatively high Feammox rates occurred during the spring tides (Figure 2). Furthermore, although the Feammox rates in the intertidal sediments were slightly different in winter and summer, a significant seasonal difference in the

contributions of Feammox to the total nitrogen loss was observed ($P < 0.05$). The relatively high Feammox contribution to nitrogen loss in winter sediments was likely attributed to the low denitrification rates that occurred during this season. Overall, these results suggested that Feammox plays an important role in NH_4^+ removal from intertidal wetlands.

Based on the potential rates of Feammox measured during the incubation experiments, the potential nitrogen loss via Feammox from the intertidal sediments was estimated at 11.5–18 t N km^{-2} year^{-1} , assuming that the dry sediment bulk density of the study area was approximately 2.68 g cm^{-3} .³ This amount of nitrogen removal via Feammox represented approximately 3.1–4.9% of the total external IN transported annually into the Yangtze Estuary wetland (approximately 366.67 t N km^{-2} year^{-1}).²¹ However, the environmental importance of Feammox in intertidal wetlands remains uncertain because anaerobic organic matter degradation and anaerobic methane oxidation can also contribute to Fe(III) reduction.^{5,37,42,43} In this study, only 1.58–3.16% of Fe(III) reduction was attributed to Feammox during the isotopic tracer incubations, based on a theoretical ratio of 3–6 mol of Fe(III) reduced per mole of NH_4^+ oxidized.^{5,18}

In summary, this study provides experimental evidence for the occurrence of Feammox in intertidal wetlands influenced by spring and neap tidal fluctuations. Tidal action can contribute to the growth of iron-reducing bacteria, which would accelerate Feammox activity and lead to more N loss from intertidal wetlands to the atmosphere. A loss of 11.5–18 t N km^{-2} year^{-1} was linked to Feammox and accounted for approximately 3.1–4.9% of the total external IN load transported annually into the Yangtze Estuary wetland. Tidal fluctuations are an important driver shaping sedimentary microenvironments and can regulate N loss through Feammox and provide new insights into Fe-driven microbial N transformations in intertidal ecosystems.

■ ASSOCIATED CONTENT

Supporting Information

The Supporting Information is available free of charge on the ACS Publications website at DOI: 10.1021/acs.est.5b03419.

Supplementary methods, figures, and tables (PDF)

■ AUTHOR INFORMATION

Corresponding Authors

*Phone: 86-21-62231669; fax: 86-21-62546441; e-mail: ljhou@sklec.ecnu.edu.cn.

*Phone: 86-21-62231669; fax: 86-21-62546441; e-mail: mliu@geo.ecnu.edu.cn.

Author Contributions

[§]X.L. and L.H. contributed equally to this work.

Notes

The authors declare no competing financial interest.

■ ACKNOWLEDGMENTS

This work was together funded by the National Natural Science Foundation of China (Nos. 41322002, 41130525, 41271114, and 41071135), the Program for New Century Excellent Talents in University (NCET), and the State Key Laboratory of Estuarine and Coastal Research. Great thanks are given to Wayne Gardner and anonymous reviewers for their constructive suggestions on earlier versions of this manuscript.

■ REFERENCES

- (1) Seitzinger, S. Nitrogen cycle: Out of reach. *Nature* **2008**, *452*, 162–163.
- (2) Galloway, J. N.; Townsend, A. R.; Erisman, J. W.; Bekunda, M.; Cai, Z.; Freney, J. R.; Martinelli, L. A.; Seitzinger, S. P.; Sutton, M. A. Transformation of the nitrogen cycle: Recent trends, questions, and potential solutions. *Science* **2008**, *320*, 889–892.
- (3) Yin, G. Y.; Hou, L. J.; Liu, M.; Liu, Z. F.; Gardner, W. S. A novel membrane inlet mass spectrometer method to measure $^{15}\text{NH}_4^+$ for isotope-enrichment experiments in aquatic ecosystems. *Environ. Sci. Technol.* **2014**, *48*, 9555–9562.
- (4) Cui, S. H.; Shi, Y. L.; Groffman, P. M.; Schlesinger, W. H.; Zhu, Y. G. Centennial-scale analysis of the creation and fate of reactive nitrogen in China (1910–2010). *Proc. Natl. Acad. Sci. U.S.A.* **2013**, *110*, 2052–2057.
- (5) Ding, L. J.; An, X. L.; Li, S.; Zhang, G. L.; Zhu, Y. G. Nitrogen loss through anaerobic ammonium oxidation coupled to iron reduction from paddy soils in a chronosequence. *Environ. Sci. Technol.* **2014**, *48*, 10641–10647.
- (6) Booth, M. S.; Campbell, C. Spring nitrate flux in the Mississippi river basin: A landscape model with conservation applications. *Environ. Sci. Technol.* **2007**, *41*, 5410–5418.
- (7) Hou, L. J.; Yin, G. Y.; Liu, M.; Zhou, J. L.; Zheng, Y. L.; Gao, J.; Zong, H. B.; Yang, Y.; Gao, L.; Tong, C. F. Effects of sulfamethazine on denitrification and the associated N_2O release in estuarine and coastal sediments. *Environ. Sci. Technol.* **2015**, *49*, 326–333.
- (8) Deegan, L. A.; Johnson, D. S.; Warren, R. S.; Peterson, B. J.; Fleeger, J. W.; Fagherazzi, S.; Wollheim, W. M. Coastal eutrophication as a driver of salt marsh loss. *Nature* **2012**, *490*, 388–392.
- (9) Ramirez, K. S.; Craine, J. M.; Fierer, N. Consistent effects of nitrogen amendments on soil microbial communities and processes across biomes. *Global Change Biol.* **2012**, *18*, 1918–1927.
- (10) Neubacher, E. C.; Parker, R. E.; Trimmer, M. Short-term hypoxia alters the balance of the nitrogen cycle in coastal sediments. *Limnol. Oceanogr.* **2011**, *56*, 651–665.
- (11) Spott, O.; Russow, R.; Stange, C. F. Formation of hybrid N_2O and hybrid N_2 due to codenitrification: First review of a barely considered process of microbially mediated N-nitrosation. *Soil Biol. Biochem.* **2011**, *43*, 1995–2011.
- (12) Kuypers, M. M. M.; LaviK, G.; Woebken, D.; Schmid, M.; Fuchs, B. M.; Amann, R.; Jørgensen, B. B.; Jetten, M. S. M. Massive nitrogen loss from the Benguela upwelling system through anaerobic ammonium oxidation. *Proc. Natl. Acad. Sci. U. S. A.* **2005**, *102*, 6478–6483.
- (13) Schubert, C. J.; Durisch-kaiser, E.; Wehrli, B.; Thamdrup, B.; Lam, P.; Kuypers, M. M. M. Anaerobic ammonium oxidation in a tropical freshwater system (Lake Tanganyika). *Environ. Microbiol.* **2006**, *8*, 1857–1863.
- (14) Long, A.; Heitman, J.; Tobias, C.; Philips, R.; Song, B. Cooccurring anammox, denitrification, and codenitrification in agricultural soils. *Appl. Environ. Microbiol.* **2013**, *79*, 168–176.
- (15) Penton, C.; Devol, A.; Tiedje, J. Molecular evidence for the broad distribution of anaerobic ammonium-oxidizing bacteria in freshwater and marine sediments. *Appl. Environ. Microbiol.* **2006**, *72*, 6829–6832.
- (16) Dale, O. R.; Tobias, C. R.; Song, B. Biogeographical distribution of diverse anaerobic ammonium oxidizing (anammox) bacteria in Cape Fear River Estuary. *Environ. Microbiol.* **2009**, *11*, 1194–1207.
- (17) Engström, P.; Dalsgaard, T.; Hulth, S.; Aller, R. C. Anaerobic ammonium oxidation by nitrite (anammox): Implications for N_2 production in coastal marine sediments. *Geochim. Cosmochim. Acta* **2005**, *69*, 2057–2065.
- (18) Yang, W. H.; Weber, K. A.; Silver, W. L. Nitrogen loss from soil through anaerobic ammonium oxidation coupled to iron reduction. *Nat. Geosci.* **2012**, *5*, 538–541.
- (19) Clément, J. C.; Shrestha, J.; Ehrenfeld, J. G.; Jaffé, P. R. Ammonium oxidation coupled to dissimilatory reduction of iron under anaerobic conditions in wetland soils. *Soil Biol. Biochem.* **2005**, *37*, 2323–2328.

- (20) Shrestha, J.; Rich, J.; Ehrenfeld, J.; Jaffe, P. Oxidation of ammonium to nitrite under iron-reducing conditions in wetland soils: Laboratory, field demonstrations, and push–pull rate determination. *Soil Sci.* **2009**, *174*, 156–164.
- (21) Hou, L. J.; Zheng, Y. L.; Liu, M.; Gong, J.; Zhang, X. L.; Yin, G. Y.; You, L. L. Anaerobic ammonium oxidation (anammox) bacterial diversity, abundance, and activity in marsh sediments of the Yangtze Estuary. *J. Geophys. Res.: Biogeosci.* **2013**, *118*, 1237–1246.
- (22) Kirwan, M. L.; Megonigal, J. P. Tidal wetland stability in the face of human impacts and sea-level rise. *Nature* **2013**, *504*, 53–60.
- (23) Vieillard, A. M.; Fulweiler, R. W. Tidal pulsing alters nitrous oxide fluxes in a temperate intertidal mudflat. *Ecology* **2014**, *95*, 1960–1971.
- (24) Li, X. F.; Hou, L. J.; Liu, M.; Lin, X. B.; Li, Y.; Li, S. W. Primary effects of extracellular enzyme activity and microbial community on carbon and nitrogen mineralization in estuarine and tidal wetlands. *Appl. Microbiol. Biotechnol.* **2015**, *99*, 2895–2909.
- (25) Sakamaki, T.; Nishimura, O.; Sudo, R. Tidal time-scale variation in nutrient flux across the sediment–water interface of an estuarine tidal flat. *Estuarine, Coastal Shelf Sci.* **2006**, *67*, 653–663.
- (26) Ardón, M.; Morse, J. L.; Colman, B. P.; Bernhardt, E. S. Drought–induced saltwater incursion leads to increased wetland nitrogen export. *Global Change Biol.* **2013**, *19*, 2976–2985.
- (27) Hou, L. J.; Liu, M.; Ding, P. X.; Zhou, J. L.; Yang, Y.; Zhao, D.; Zheng, Y. L. Influences of sediment dessication on phosphorus transformations in an intertidal marsh: Formation and release of phosphine. *Chemosphere* **2011**, *83*, 917–924.
- (28) Liu, Z. F.; Lee, C. Drying effects on sorption capacity of coastal sediment: the importance of architecture and polarity of organic matter. *Geochim. Cosmochim. Acta* **2006**, *70*, 3313–3324.
- (29) Tang, Y. S.; Wang, L.; Jia, J. W.; Li, Y. L.; Zhang, W. Q.; Wang, H. L.; Sun, Y. Response of soil microbial respiration of tidal wetlands in the Yangtze River Estuary to different artificial disturbances. *Ecol. Eng.* **2011**, *37*, 1638–1646.
- (30) Chen, X.; Zong, Y. Coastal erosion along the Changjiang deltaic shoreline, China: History and prospective. *Estuarine, Coastal Shelf Sci.* **1998**, *46*, 733–742.
- (31) Lovley, D. R.; Phillips, E. J. P. Rapid assay for microbially reducible ferric iron in aquatic sediments. *Appl. Environ. Microbiol.* **1987**, *53*, 1536–1540.
- (32) Somenahally, A. C.; Hollister, E. B.; Yan, W.; Gentry, T. J.; Loeppert, R. H. Water management impacts on arsenic speciation and iron-reducing bacteria in contrasting rice-rhizosphere compartments. *Environ. Sci. Technol.* **2011**, *45*, 8328–8335.
- (33) Santos, I. R.; Cook, P. L.; Rogers, L.; Weys, J. d.; Eyre, B. D. The “salt wedge pump”: Convection–driven pore–water exchange as a source of dissolved organic and inorganic carbon and nitrogen to an estuary. *Limnol. Oceanogr.* **2012**, *57*, 1415–1426.
- (34) Bullock, A. L.; Sutton-Grier, A. E.; Megonigal, J. P. Anaerobic metabolism in tidal freshwater wetlands. III. Temperature regulation of iron cycling. *Estuaries Coasts* **2013**, *36*, 482–490.
- (35) Caffrey, J. M.; Bano, N.; Kalanetra, K.; Hollibaugh, J. T. Ammonia oxidation and ammonia-oxidizing bacteria and archaea from estuaries with differing histories of hypoxia. *ISME J.* **2007**, *1*, 660–662.
- (36) Burton, E. D.; Bush, R. T.; Johnston, S. G.; Sullivan, L. A.; Keene, A. F. Sulfur biogeochemical cycling and novel Fe–S mineralization pathways in a tidally re-flooded wetland. *Geochim. Cosmochim. Acta* **2011**, *75*, 3434–3451.
- (37) Kostka, J. E.; Gribsholt, B.; Petrie, E.; Dalton, D.; Skelton, H.; Kristensen, E. The rates and pathways of carbon oxidation in bioturbated saltmarsh sediments. *Limnol. Oceanogr.* **2002**, *47*, 230–240.
- (38) Weber, K. A.; Achenbach, L. A.; Coates, J. D. Microorganisms pumping iron: anaerobic microbial iron oxidation and reduction. *Nat. Rev. Microbiol.* **2006**, *4*, 752–764.
- (39) Nevin, K. P.; Lovley, D. R. Lack of production of electron-shuttling compounds or solubilization of Fe(III) during reduction of insoluble Fe(III) oxide by *Geobacter metallireducens*. *Appl. Environ. Microbiol.* **2000**, *66*, 2248–2251.
- (40) Scheid, D.; Stubner, S.; Conrad, R. Identification of rice root associated nitrate, sulfate and ferric iron reducing bacteria during root decomposition. *FEMS Microbiol. Ecol.* **2004**, *50*, 101–110.
- (41) King, G. M.; Garey, M. A. Ferric iron reduction by bacteria associated with the roots of freshwater and marine macrophytes. *Appl. Environ. Microbiol.* **1999**, *65*, 4393–4398.
- (42) Lovley, D. R.; Phillips, E. J. P. Organic matter mineralization with reduction of ferric iron in anaerobic sediments. *Appl. Environ. Microbiol.* **1986**, *51*, 683–689.
- (43) Teh, Y. A.; Dubinsky, E.; Silver, W.; Carlson, C. M. Suppression of methanogenesis by dissimilatory Fe(III)-reducing bacteria in tropical rain forest soils: Implications for ecosystem methane flux. *Global Change Biol.* **2008**, *14*, 413–422.
- (44) Jensen, M. M.; Thamdrup, B.; Dalsgaard, T. Effects of specific inhibitors on anammox and denitrification in marine sediments. *Appl. Environ. Microbiol.* **2007**, *73*, 3151–3158.
- (45) Sorensen, J. Denitrification rates in a marine sediments as measured by the acetylene inhibition technique. *Appl. Environ. Microbiol.* **1978**, *36*, 139–143.